JOURNAL OF MATERIALS SCIENCE 28 (1993) 2148–2156

Tensile stress–strain behaviour of cementitious composites at high loading rates

M. A. GLINICKI
Institute of Fundamental Technological Research, Polish Academy of Sciences, Świętokrzyska 21, PL- 00-049 Warsaw, Poland

The influence of loading rate on the tensile stress–strain behaviour of cementitious composites was studied experimentally. The project was undertaken to obtain an insight into the possible relation between internal structure parameters of composites and their loading-rate sensitivity. Five different types of cementitious composites were applied. Composite structure data were obtained by testing porosity and by quantitative observation of fracture surfaces. Direct tensile tests were performed at four different loading rates within the range 0.001–1000 MPa s^{-1}. The tensile stress–strain behaviour was significantly influenced by the loading rate and structure parameters of composites. The relative tensile strength increase due to an increase of loading rate was found to be higher for composites with higher total porosity. Recorded stress–strain diagrams obtained at various loading rates are presented and discussed with the aid of continuous damage mechanics.

1. Introduction

The rational assessment of the structural response due to suddenly applied loads requires the realistic modelling of the material behaviour at high rates of stress. The loading-rate sensitive behaviour of concrete in tension has been under investigation for several years [1–3]. However, a number of questions have remained unanswered and knowledge concerning dynamic properties of modern cementitious composites is still incomplete.

The loading-rate sensitivity in tension has generally been measured in terms of strength, modulus of elasticity or strain at the maximum stress (ultimate strain). It has also been measured with respect to Poisson's ratio and fracture toughness (e.g. [4, 5]). The term "loading-rate sensitivity" is used to describe effects of changes of deformation and fracture parameters induced by an increase in the loading rate, $\dot{\sigma}$. Previous studies by several investigators, recently reviewed by Banthia and Pigeon [6], have been concerned with the technological aspects of rate-induced effects. Therefore, the structural reasons underlying the loading-rate sensitivity have not been clearly identified. For example, a transmission of fracture mode from aggregate debonding to aggregate breaking is regarded as a major cause of rate-induced effects. However, no quantitative evaluation of this phenomenon has been obtained experimentally.

The purpose of this study was to obtain information concerning the influence of loading rate on the stress–strain behaviour of cementitious composites in tension. The major research task was to evaluate differences in the dynamic response of materials in relation to parameters of their internal structures. As a convenient measure of the loading-rate sensitivity, the dynamic increase factors were applied (after Ross *et al.* [7]). The dynamic increase factors are the relative increase of evaluated properties as a function of applied stress rate. The properties considered were the tensile strength, f_t, and the ultimate strain, ε_u. The following definitions of the dynamic strength increase factor (*DSIF*) and dynamic deformation increase factor (*DDIF*) are proposed

$$DSIF = \frac{f_t(\dot{\sigma})}{f_t(\dot{\sigma}_0)} \tag{1a}$$

$$DDIF = \frac{\varepsilon_u(\dot{\sigma})}{\varepsilon_u(\dot{\sigma}_0)} \tag{1b}$$

where $\dot{\sigma}$ and $\dot{\sigma}_0$ are the considered loading rate and the reference (e.g. static) loading rate, respectively. The range of tests is limited to 10^{-3} to 10^{+3} MPa s^{-1}, i.e. it covers the rates characteristic for a number of applications in engineering, including a lower part of the seismic rates spectrum.

The range of cement-based composites considered included mortar, concrete and fibre-reinforced concrete. The following structure parameters were chosen to be studied in detail: porosity, aggregate inclusion content and fibre inclusion type and content. In order to distinguish clearly the loading rate/structure change effects from the usual scatter of experimental results, the differences in structural parameters were exaggerated. Thus, the composites considered were selected from the points in the structure parameters space shown in Fig. 1.

The project reported here was concerned with assessment of structural aspects of loading-rate sensitivity of cementitious composites. The effects of loading rate on the stress–strain properties have been

0022–2461

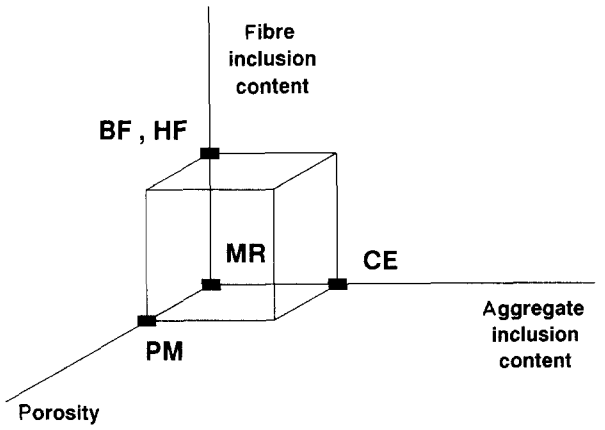

Figure 1 The concept of macrostructural parameters space for the explored range of composites.

examined in relation to internal structure parameters of cementitious composites.

2. Experimental procedure

2.1. Materials and specimens

To cover the considered range of structural parameters, the following types of composite were manufactured: mortar, macroporous mortar, model concrete and fibre-reinforced mortars. The mix proportions based on the weight of cement for each type of composite are given in Table I.

The term "model" concrete (CE), refers to the composite containing gravel particles falling within the range 8–12.5 mm. In order to imitate the existence of macropores in porous mortar (PM), an addition of polyethylene beads was used. For two fibrous composites the following steel fibre types were applied:

(i) Bekaert fibres (length 30 mm, diameter 0.4 mm) in a volume fraction of 1%, for the composite denoted BF;

(ii) Harex fibres (length 32 mm) in a volume fraction of 1.4%, for the composite denoted HF.

The mix proportions were experimentally determined in each case, provided that the type of cement, sand, as well as manufacturing and curing conditions, were the same. The major requirements for mix design were: the same workability of mix (Ve–Be time 5–12 s); the same class of composites being understood as materials of the same static tensile strength.

Test specimens were "paddle-shaped" (Fig. 2) with a cross-section of 45 mm × 100 mm. The total length of the specimen was 490 mm. The specimens were cast horizontally, demoulded after 2 days and then kept in a humid room until testing. Prior to testing, the specimens were notched in the middle with two 17 mm notches from each side. For each type of composite material, 20 specimens were cast and tested.

2.2. Testing procedure

Direct tensile tests were carried out on an Instron 1205 testing machine using special grips for specimens

TABLE I The mix proportions

	Composite			
	MR	PM	CE	BF/HF
Cement	1	1	1	1
Sand	3.7	2.0	3.5	4.1
Gravel			2.3	
Water	0.5	0.4	0.5	0.6

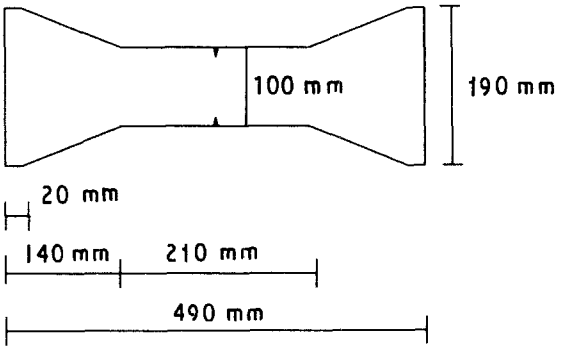

Figure 2 The test specimen.

(Fig. 3a). For the performance of four distinct series of tests, a crosshead displacement control was chosen. The control parameters were selected so as to obtain the following average loading rates: 0.002, 1, 50 and 900 MPa s^{-1}. During tensile testing the following measurements were taken: the load output from the load cell, the axial strain of the specimen obtained by means of strain gauges, and axial deformation of the specimen at both sides as measured using a LVDT transducer. Fig. 3b shows a flow chart of a measuring system. A high-speed digital recording system (8 kilo words/channel) enabled simultaneous monitoring of measured signals in time. In the case of the lowest rate tests, some analogue XY recorders were additionally applied. Permanent storage of the data, as well as further analysis, was accomplished using a personal computer.

The structure parameters of the composites were evaluated after fracture of the specimens. Quantitative observation of fracture surfaces and a digital image analyser provided data on the number of fibres, the number and surface fraction of aggregate particles, as well as macropores. For all types of composite, both density and porosity evaluation were also performed.

3. Results

Typical data records obtained from direct tensile tests at different loading rates are presented in Figs 4 and 5. The results consist of average tensile stress, σ, axial strain, ε, axial deformation at both sides of specimen, δ_w and δ_x, as a function of time. As is noticed the observed range of load rise times was between about 4 ms and 30 min. The record of average tensile stress with time enables a precise determination of actual applied loading rate. It should be kept in mind that

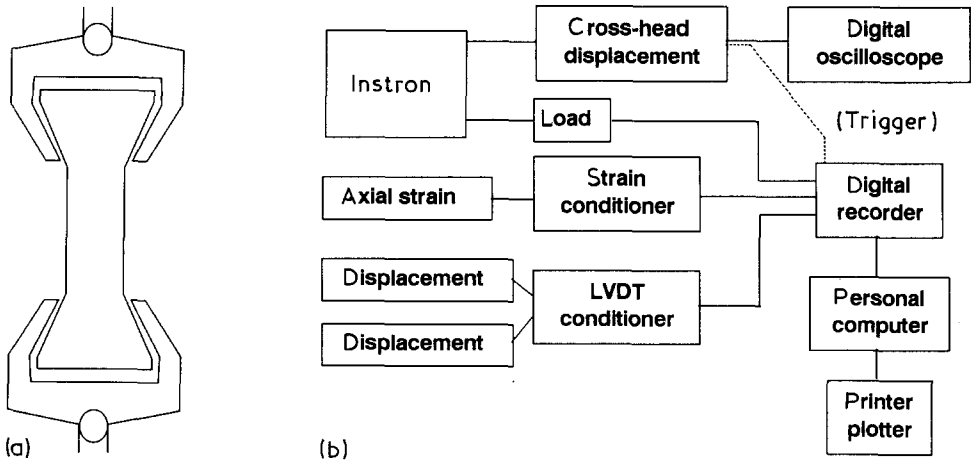

Figure 3 The testing arrangement.

TABLE II The tensile strength, f_t, and ultimate strain, ε_u for all tested composites

Type of composite	Designation	Loading rate (MPa s^{-1})							
		0.002		1.0		50		900	
		f_t (MPa)	ε_u (10^{-6})	f_t (MPa)	ε_u (10^{-6})	f_t (MPa)	ε_u (10^{-6})	f_t (MPa)	ε_u (10^{-6})
Plain mortar	MR	1.72 (0.13)	88 (17)	1.79 (0.11)	97 (16)	2.44 (0.11)	124 (13)	3.65 (0.26)	175 (15)
Porous mortar	PM	1.73 (0.22)	120 (19)	1.77 (0.15)	110 (23)	2.50 (0.21)	150 (42)	3.94 (0.51)	184 (14)
Model concrete	CE	2.20 (0.22)	122 (18)	2.43 (0.32)	116 (17)	2.82 (0.30)	127 (19)	3.41 (0.33)	193 (10)
Bekaert fibre mortar	BF	1.80 (0.14)	141 (31)	2.00 (0.42)	142 (21)	2.51 (0.45)	163 (14)	3.44 (0.32)	186 (17)
Harex fibre mortar	HF	1.84 (0.16)	162 (30)	1.92 (0.17)	153 (64)	2.38 (0.19)	213 (55)	3.09 (0.19)	325 (63)

the loading rate was not a control (input) parameter for the loading process – it was a result of a kinematically controlled procedure. The loading process up to about the maximum load, can be fairly well characterized by a constant loading rate, $\dot{\sigma}$. The presented experimental data were also used in the evaluation of the tensile strength and the ultimate strain and to obtain stress–strain relationships.

The attained values of the tensile strength, f_t, and the ultimate strain, ε_u, of cementitious composites are given in Table II. These are the average values of 4–6 specimens and the numbers in brackets are standard deviations. It should be noted that the intended requirement of the same static tensile strength of tested composites could be fulfilled with a fairly good fit; f_t for all the tested series of specimens was between 1.72 and 2.20 MPa. The obtained results will be discussed in relation to the composite structure parameters given below.

The results of total porosity estimation are presented in Table III. These are the average values of six samples for each type of composite. In the case of PM composite, the effect of artificially induced porosity has also been accounted for. It is noted that the total porosity of the composites varied significantly, ranging from 0.15–0.28.

TABLE III Total porosity of tested composites

	Composite				
	MR	PM	CE	BF	HF
Porosity	0.22	0.28	0.15	0.21	0.19

Some interesting observations of specimen fracture surfaces are given below. For fibre-reinforced composites the number of fibres was counted and expressed in terms of the number of fibres over the surface area of 1 cm^2 (N_A^f) . It was found that $N_A^f = 1.78 - 3.54$ cm^2 for Bekaert fibre composite (BF) and $N_A^f = 1.00 - 2.24$ cm^2 for Harex fibre composite (HF). Using the concept of idealized fibre distribution, the following differences in actual distribution could be recognized. The average value of N_A^f for HF was quite close to the value predicted for an ideal spatial

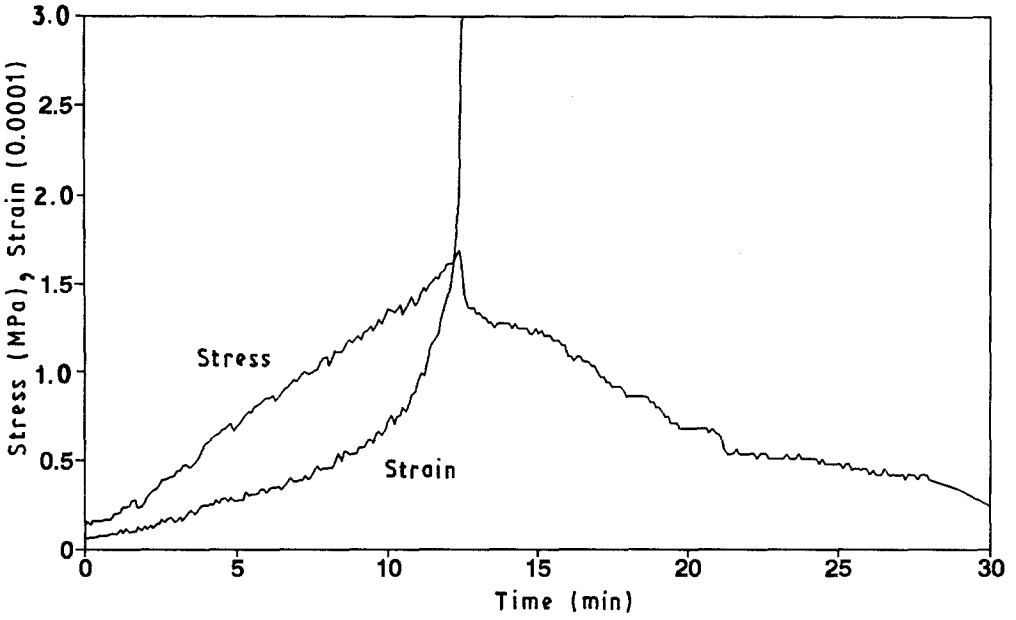

Figure 4 Example of data record obtained in quasi-static series. HF 7T, 0.002 MPa s^{-1}.

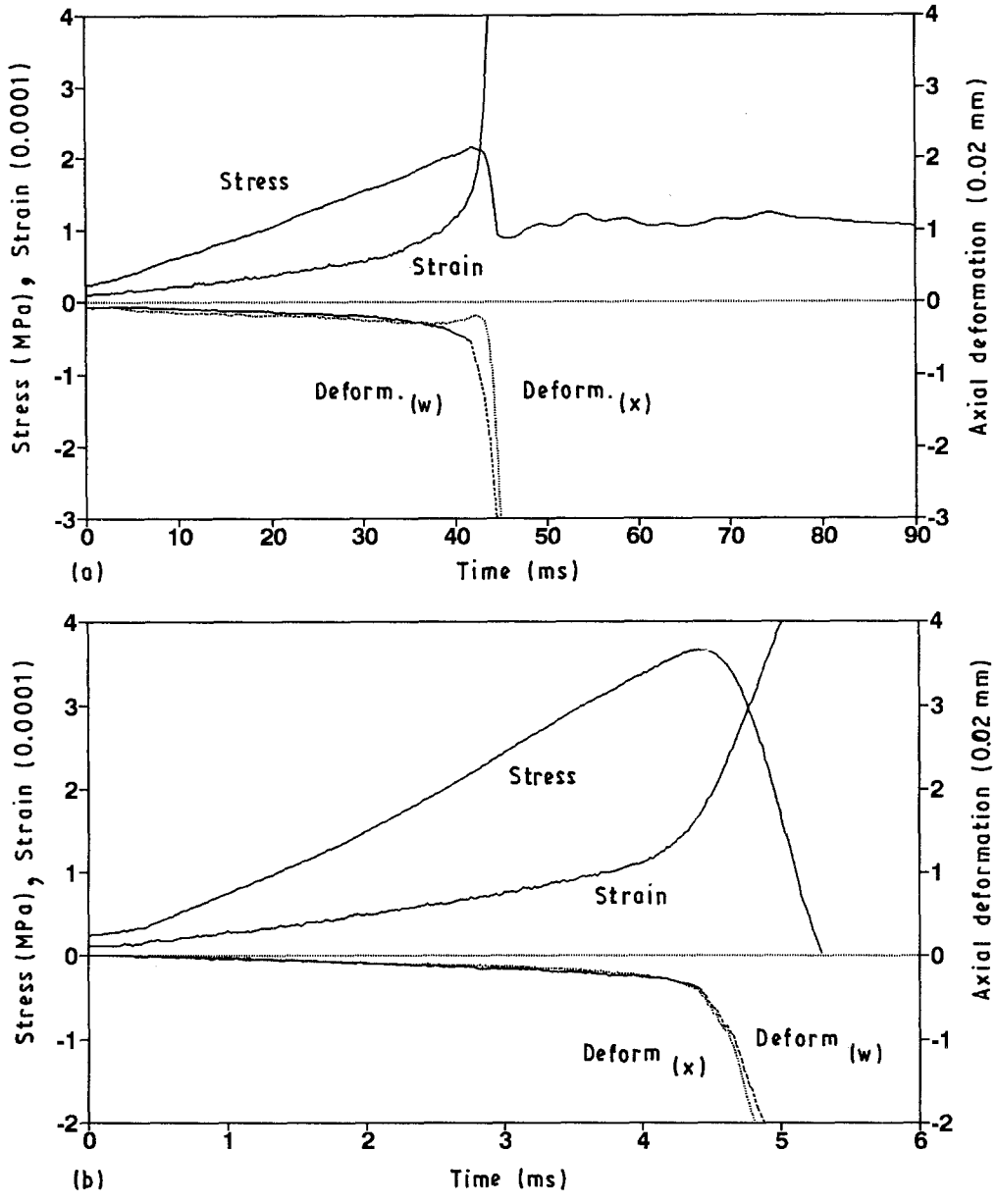

Figure 5 Examples of data records obtained with different rate of loading. (a) BF 13B, 47 MPa s^{-1}; (b) MR 20B, 900 MPa s^{-1}.

random-fibre distribution. For BF composite, an intermediate distribution, i.e. between random spatial and plane, was observed. The indicated plane was the plane parallel to the casting direction. Similar orientation effects were reported by Körmeling [8] and Babut [9]; however the reasons for them remain unknown.

The fracture surface analysis of CE composites concerned the fraction of debonded and cracked-through aggregates. Dimensionless parameters of content of debonded aggregate particles and fractured particles relative to the total fractured surface were denoted A_A^{ab} and A_A^{ac}, respectively. The loading-rate influence upon parameters A_A^{ab} and A_A^{ac} is illustrated in Fig. 6. The continuous lines are used to connect the average values at each loading rate series. It is noted that no significant influence on the fraction of debonded as well as cracked aggregate particles was observed. Therefore, a possible explanation of loading-rate effects based on a higher content of fractured aggregates (e.g. [10, 11]) is not applicable in the reported case.

4. Analysis and discussion

An analysis of the data, summarized in Table II,

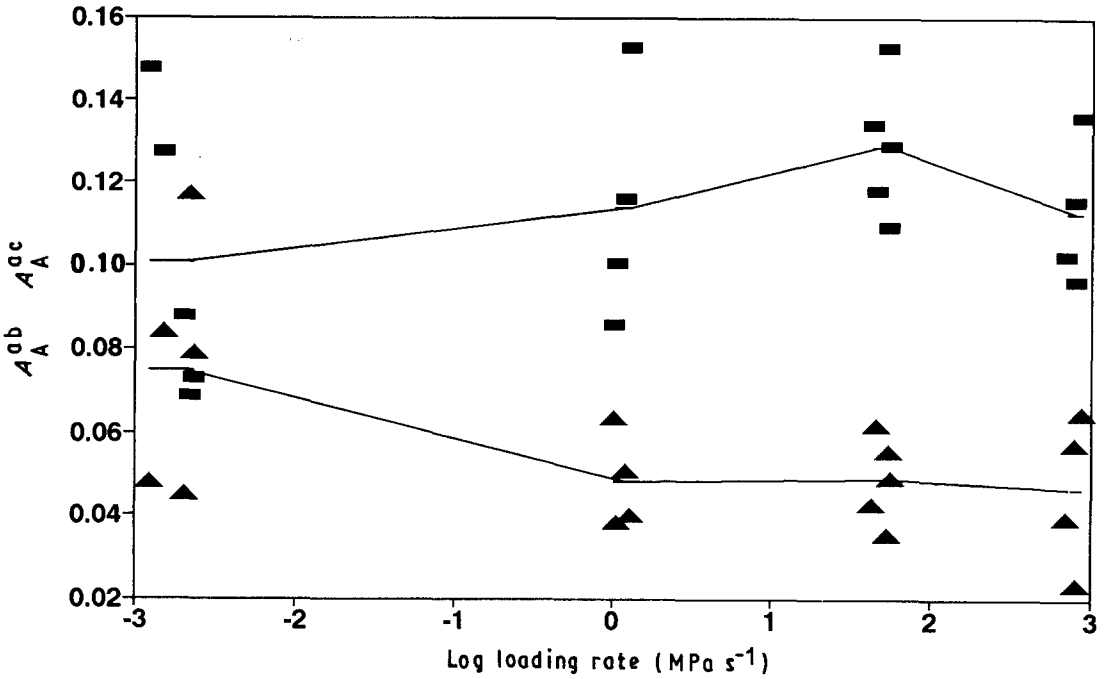

Figure 6 The relative area of (■) fractured, A_A^{ac} and (▲) debonded, A_A^{ab}, aggregate particles, for a model concrete.

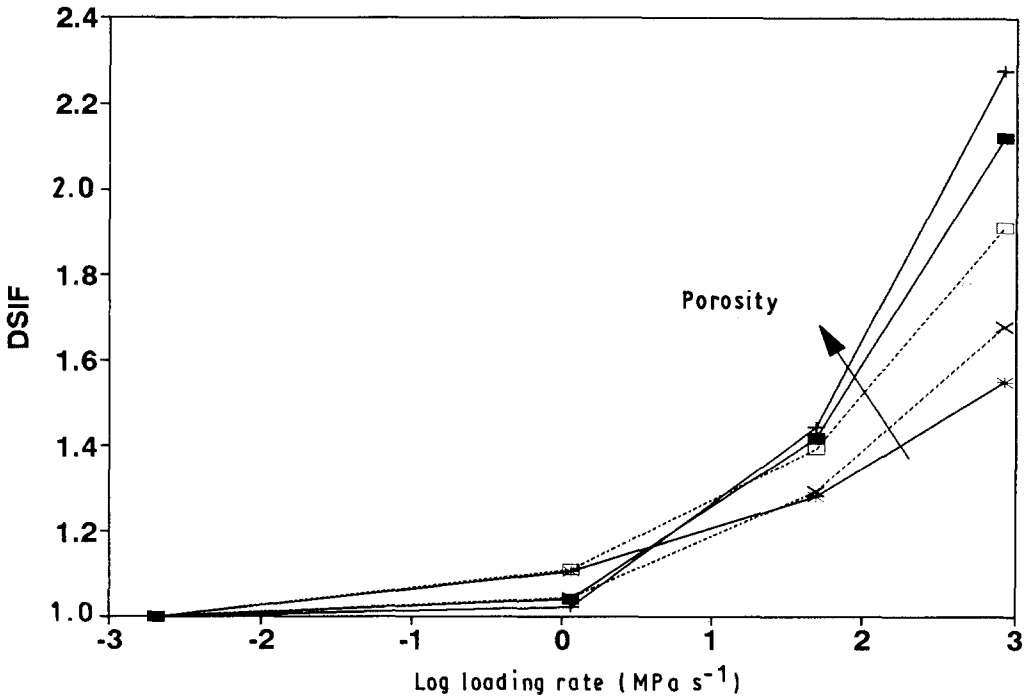

Figure 7 Relative increase in the tensile strength of composites, expressed as DSIF, versus the loading rate. (■) MR mortar, (+) PM mortar, (∗) CE model concrete, (□) BF Bekaert f. mortar, (×) HF Harex f. mortar.

revealed a significant influence of applied loading rate upon the tensile behaviour of composites. As illustrated in Fig. 7, the average tensile strength of composites progressively increases for increasing loading rates. The term "progressively" is used to indicate highly non-linear increase, even if a double logarithmic scale is considered. The best fit to the results obtained provided the following formula for the dynamic strength increase factor (*DSIF*)

$$DSIF = 1 + \alpha\left(\frac{\dot{\sigma}}{\dot{\sigma}_0}\right)^{\beta} \quad (2)$$

where $\dot{\sigma}$ and $\dot{\sigma}_0$ are the actual loading rate and the reference (e.g. static) loading rate respectively, α and β are material parameters.

It should be noted that the *DSIF* values were significantly different for the composites tested, especially in the range of highest loading rates. A remarkable observation is that over the explored range of $\dot{\sigma}$, the increase in *DSIF* was related to the total porosity of the composites. A linear regression analysis yielded the relationships between the material parameters α and β used in Equation 2, and the total porosity, p. The relationships obtained are illustrated in Fig. 8. In addition, this figure contains information about the regression coefficients.

The results indicate that a relative tensile strength increase due to an increase in loading rate is higher for composites with higher porosity. Referring to the studies published by other authors, no such *DSIF*–porosity relationship could be found; however, indirect experimental evidence can be recalled to support it. A higher loading-rate sensitivity, i.e. f_t, was however reported for lower quality concrete, higher w/c ratio, and these technological parameters could imply a higher porosity of materials. Further evidence, given by Darvin *et al.* [12] was deduced from the results for mortar with and without the addition of silica fume. The addition of silica fume was found to decrease the loading-rate sensitivity; however, the observation was gained in compression not in tension. It can be concluded that the heterogeneity of composite structure determined by the porosity can be the major reason for the rate-induced increase of the tensile strength of composites.

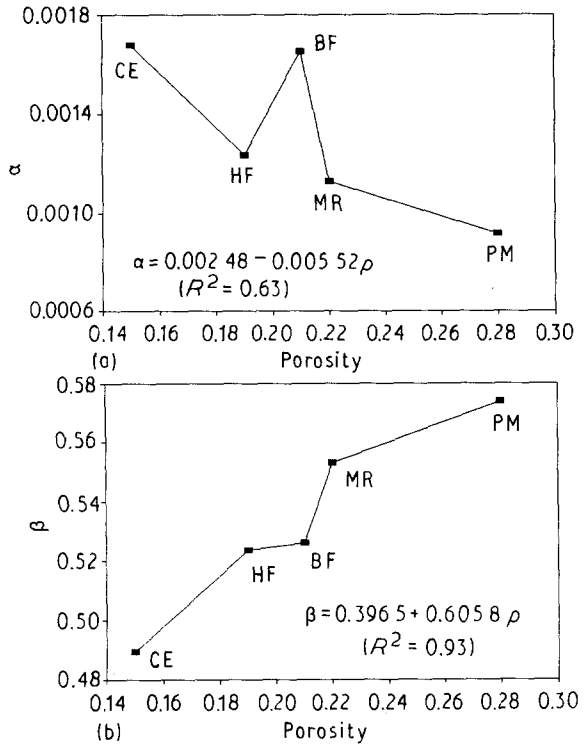

Figure 8 Relationships between coefficients (a) α and (b) β from Equation 2 and porosity of composites.

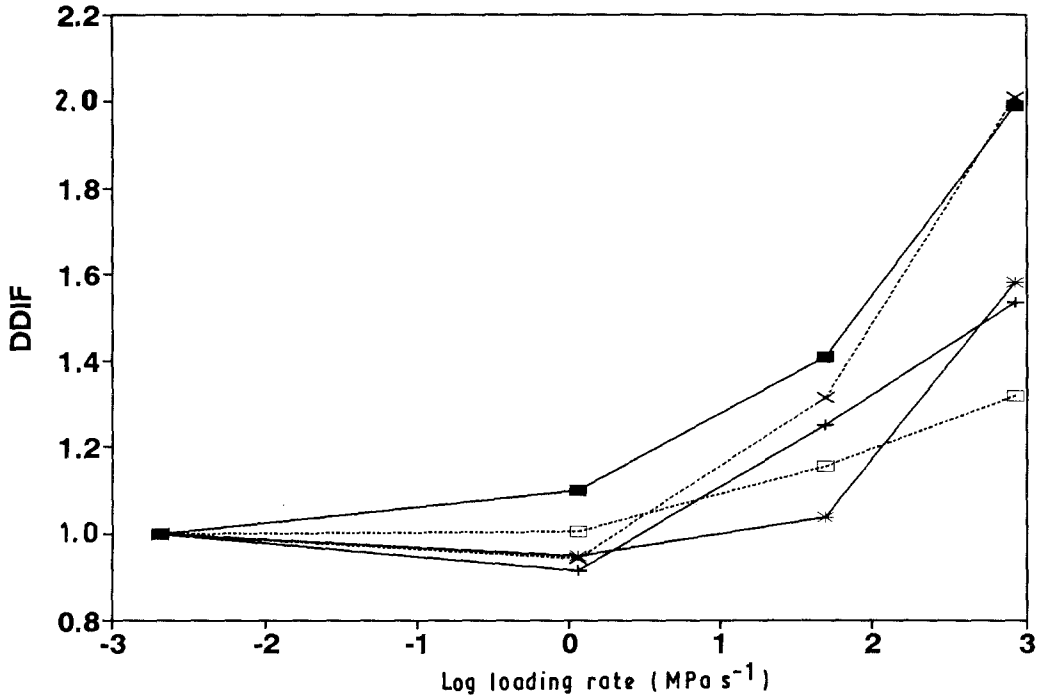

Figure 9 Relative increase in the ultimate strain of composites, expressed as DDIF, versus the loading rate. (■) MR mortar, (+) PM mortar, (∗) CE model concrete, (□) BF Bekaert f. mortar, (×) HF Harex f. mortar.

The ultimate strain can be considered in a macroscopic sense as a limiting value separating a material continuum state and fracture state that occurs as a result of coalescence of microcracks eventually forming a macrocrack. The given definition of ε_u becomes rather questionable for fibre-reinforced composites, because this strain includes apparently existing cracks. However, the range of investigation has not included high fibre contents, so the ε_u value can be fairly well regarded as a reversibility limit for the whole range of tested materials. An illustration of the loading-rate effect on an increase in average ultimate strain for tested composites is given in Fig. 9.

The observed relationships are not strictly monotonic, as in the case of the tensile strength. No significant increase or rather a slight decrease of ε_u was noticed while increasing $\dot{\sigma}$ from 10^{-3} MPa s^{-1} to 10^{0} MPa s^{-1}. A further increase in the loading rate clearly resulted in an increase in *DDIF* up to 2.0. Referring to the data published by Körmeling [8], some differences for fibre-reinforced composites could be deduced. The composite reinforced with Harex fibres showed significantly higher rate sensitivity in terms of ε_u than Bekaert fibre composite. Contrary to Körmeling's results, no relation between the number of fibres in fracture surfaces and *DDIF* was observed, irrespective of fibre type. However, to explain the differences in the loading-rate sensitivity in terms of ε_u, the observations of fibre distribution should be recalled. It was stated previously that the orientation of fibrous reinforcement in relation to the tensile load direction was less effective for Bekaert fibres than for Harex fibres. A similar tendency could be deduced from the data given by Rostasy and Hartwich [13],

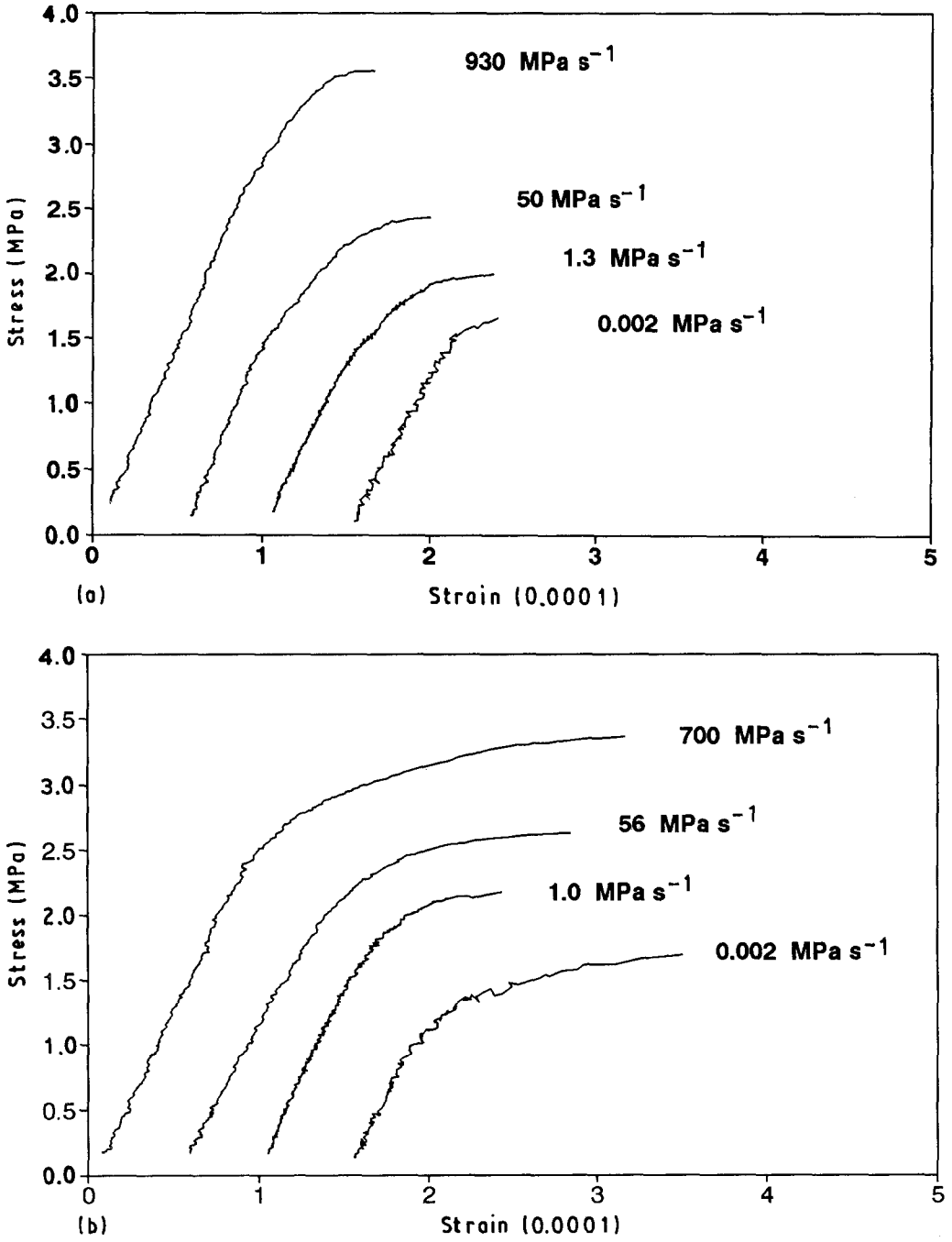

Figure 10 Examples of stress–strain relationships for two types of composites obtained at various loading rates. (a) PM, (b) HF.

although obtained for a much narrower range of loading rates.

Some examples of stress–strain curves for two types of composites are given in Fig. 10. It can be noticed that these typical curves obtained at different loading rates have certain common features. The σ–ε curves become less non-linear as the loading rate increases, thus the characteristic becomes closer to linear within the wider range of strain. This can be understood as a decrease of microcracking or as a reduction of sub-critical flaw growth at high loading rates. Such a qualitative interpretation was offered by, for example, Banthia *et al.* [14]; however, a quantitative evaluation of observations still calls for further attention.

To quantify the differences in the σ–ε diagrams due to an increase of the loading rate, the concept of continuous damage was used. Following the basic research on continuous damage mechanics (e.g. [15]) a damage variable, ω, was introduced. For the sake of simplicity the variable ω is considered as a scalar, i.e. the following definition was used.

$$\omega = \begin{cases} 0 & \text{for } \varepsilon = 0 \\ 1 - \sigma/(E_0\varepsilon) & \text{for } \varepsilon > 0 \end{cases} \quad (3)$$

where σ denotes the stress, ε the strain and E_0 the initial modulus of deformation. Thus the damage is defined as the area density of voids in a given cross-section. The damage is treated as a kinematic variable, the growth of which results in the gradual degradation of the material. According to the given definition, $0 \leqslant \omega \leqslant 1$, i.e. the stage of no load-carrying capability is determined by $\omega = 1$.

Using the experimental records of the stress and strain with time, a precise determination of the damage evolution for each tested specimen was possible according to Equation 3. An example of the damage evolution for a specimen in a high rate test is shown in Fig. 11. Apart from experimental data, a fitted exponential curve is also shown.

The curve shown was cut at the point corresponding to the "ultimate moment" in the loading process, i.e. the moment when the tensile strength of the material was reached. By analogy to ε_u, the damage at this point is called the ultimate damage, ω_u. An interesting observation can be made on comparing the ultimate damage for specimens tested at different loading rates. Average values of ω_u for all tested composites plotted against the loading rate are shown in Fig. 12. It is noted that no significant influence of $\dot{\sigma}$ upon the ultimate damage was found. Only in the case of Harex fibre composite was a slight increasing tendency observed. However, taking into account the scatter of the results, a general lack of clear rate dependency of ω_u can be stated. Accepting the interpretation of the damage, ω, as the density of microcracks, no quantitative experimental evidence for microcracking increase or decrease can be given. This, of course, concerns pre-critical crack growth that takes place prior to peak load.

The observations reported for damage evolution provide a basis for model interpretation of the loading-rate influence upon the tensile strength of cement composites. An elaboration of the model was described elsewhere [16]. However, further research is still required, particularly focusing on the rate dependency of fracture phenomena occurring after the peak stress.

6. Conclusions

1. The increase in the tensile strength induced by increasing loading rates is related to the total porosity of tested composites. A higher porosity implying a higher heterogeneity of composite structure produces a higher loading-rate sensitivity in terms of the tensile strength.

2. The strain at peak stress varies in a non-monotonic manner with loading rate. With increasing loading rate the ultimate strain first decreases (at about 1 MPa s^{-1}) and then significantly increases up to two-fold.

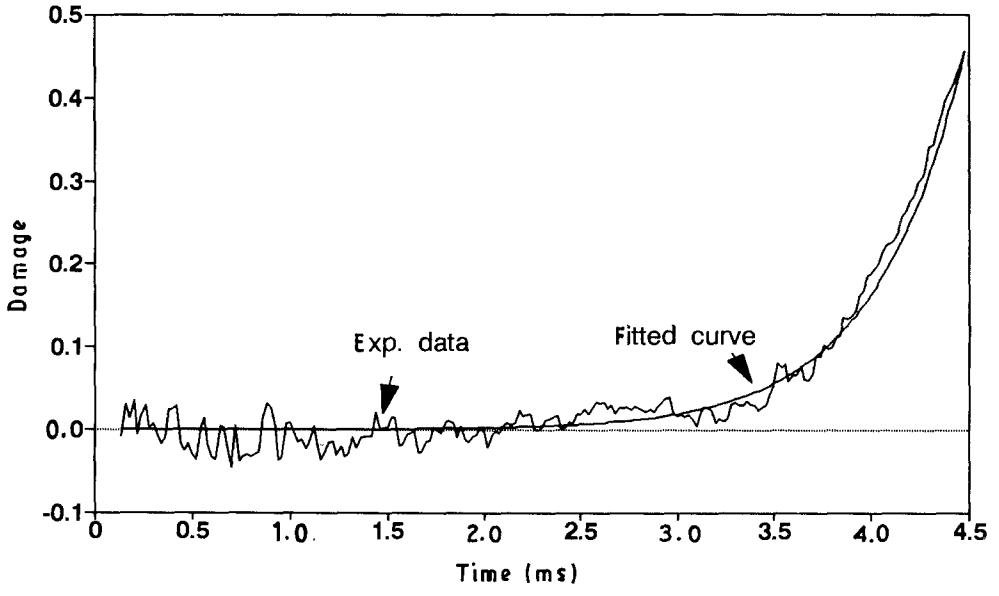

Figure 11 An example of the damage evolution for a "model concrete" (CE 23T) specimen, at 818 MPa s^{-1}.

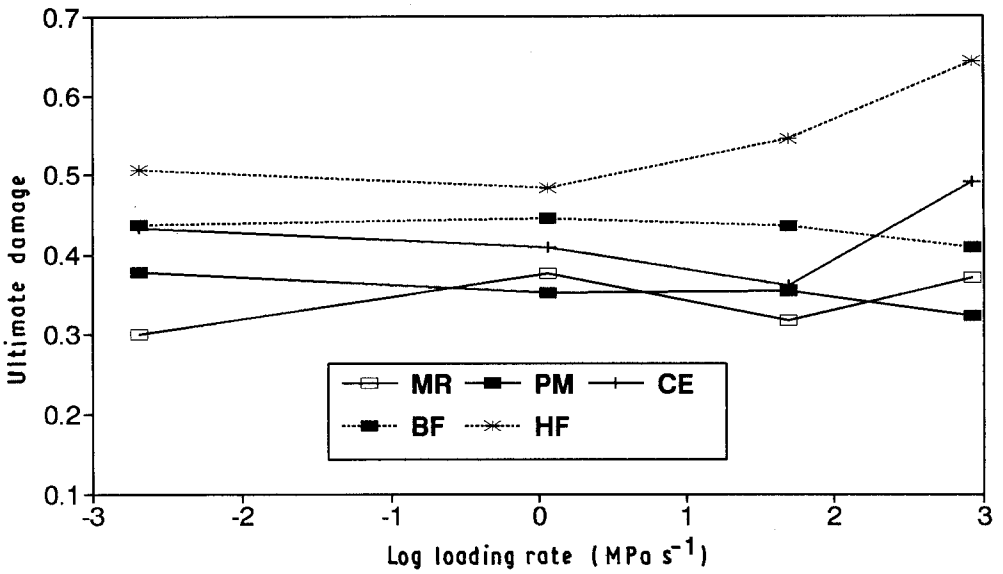

Figure 12 Relationship between the ultimate damage and the loading rate for all tested composites. (□) MR, (–■–) PM, (+) CE (- - ■ - -) BF, (∗) HF.

3. The stress–strain curves for the composites considered are non-linear, but this non-linearity decreases with increasing loading rate. However, the ultimate damage, defined as the density of microcracks at the peak load, is hardly affected by a change of loading rate.

4. No relationship between the number of fibres in the fracture surfaces and the loading-rate sensitivity in terms of f_t and ε_u is found. However, a change of fibre distribution and a difference in fibre shape influence the relative increase in the ultimate strain of fibrous composites.

5. A fracture mode varying from aggregate debonding to aggregate breaking is found to have no importance in inducing the reported rate effects. Therefore, a dominant influence can be attributed to an inertia of subcritical microcracking and possibly multiple microcracking of the material.

Acknowledgement

The author thanks Professor A. M. Brandt, IFTR, PAS, for helpful suggestions and valuable comments concerning this research project.

References

1. H. W. REINHARDT, Stevin Report 25-87-16, Delft University of Technology, Delft, The Netherlands (1987).
2. J. EIBL and M. CURBACH, in "Transactions of the 9th International Conference on SMiRT," Lausanne, Vol. H, ed F. H. Wittmann, (A. A. Balkema, Rotterdam, Boston, 1987) p. 245.
3. M. A. GLINICKI, in "Cement-Based Composites: Strain Rate Effects on Fracture", edited by S. Mindess and S. P. Shah, MRS Symposium Proceedings, Vol. 64, (MRS, Pittsburgh, PA, 1986) p. 93.
4. G. G. NAMMUR and A.E. NAAMAN, *ibid.*, p. 97.
5. M. A. GLINICKI, in "Brittle Matrix Composites 3", edited by A. M. Brandt and I. H. Marshall (Elsevier Applied Science, London, New York, 1991) p. 138.
6. N. BANTHIA and M. PIGEON, in "Structures under Shock and Impact", edited by P. S. Bulson (Elsevier/Computational Mechanics Publications, Southampton, 1989) p. 107.
7. C. A. ROSS, P.Y. THOMPSON and J.W. TEDESCO, *ACI Mater. J.* **86** (1989), 475.
8. H. A. KÖRMELING, PhD thesis, Delft University of Technology (1986).
9. R. BABUT, *Heron* **31** (2) (1986) 29.
10. E. BRÜHWILER and F. H. WITTMANN, *Engng Fract. Mech.* **35** (1990) 565.
11. A. J. ZIELINSKI, *Cement Concr. Res.* **14** (1984), 215.
12. D. DARVIN, S. ZHENJIA and S. HARSH in "Bonding in Cementitious Composites", edited by S. P. Shah and S. Mindess, MRS Symposium Proceedings, Vol. 114 (MRS, Pittsburgh, PA, 1988) p. 105.
13. F. S. ROSTASY and K. HARTWICH, Festigkeits- und Verformungsverhalten von stahlfaserbewehrtem normal Beton unter hohen und schnell ablaufenden Belastungen, Techn. Universitat Braunschweig, (1983).
14. N. BANTHIA, S. MINDESS and A. BENTUR, *Mater. Struct.* **20** (118) (1987) 293.
15. M. LORRAIN and K. E. LOLAND, in "Fracture Mechanics of Concrete", edited by F. H. Wittmann (Elsevier, Amsterdam, 1983) p. 341.
16. M. A. GLINICKI, PhD thesis, IFTR PAS, Warsaw (1991).

Received 25 November 1991
and accepted 2 September 1992